Applied and Computational Mathematics
2024; 13(5): 130-139
http://www.sciencepublishinggroup.com/j/acm
doi: 10.11648/j.acm.20241305.12
ISSN: 2328-5605 (Print); ISSN: 2328-5613 (Online)

Hydromagnetic Non-Newtonian Nanofluid Flow Past Linealy Stretching Convergent-Divergent Conduit with Chemical Reaction

Paul Wachira Githaiga, Mathew Ngugi Kinyanjui, Roy Phineas Kiogora*

Department of Pure and Applied Mathematics, Jomo Kenyatta University of Agriculture and Technology, Nairobi, Kenya

Email address:

wachipaul@gmail.com (Paul Wachira Githaiga), mathewkiny@jkuat.ac.ke (Mathew Ngugi Kinyanjui),
Prkiogora@fsc.jkuat.ac.ke (Roy Phineas Kiogora)
*Corresponding author

To cite this article:

Paul Wachira Githaiga, Mathew Ngugi Kinyanjui, Roy Phineas Kiogora. (2024). Hydromagnetic Non-Newtonian Nanofluid Flow Past Linealy Stretching Convergent-Divergent Conduit with Chemical Reaction. *Applied and Computational Mathematics, 13*(5), 130-139. https://doi.org/10.11648/j.acm.20241305.12

Received: 17 July 2024; **Accepted:** 24 August 2024; **Published:** 5 September 2024

Abstract: This paper investigates hydromagnetic non-Newtonian nanofluid flow past linearly stretching convergent-divergent conduit with chemical reaction using spectral ralaxation method. The fluid considered here is electrically conducting and is subjected to a constant pressure gradient and variable magnetic field. The two non-parallel walls are assumed not to intersect and the angle between the inclined walls is θ. The governing equations are continuity equation, momentum equation, species concentration, induction equation and energy equation. On modelling, the resulting partial differential equations are non-linear and are first transformed into system of ordinary differential equations through similarity transformation. The resulting boundary value problem is solved numerically using Spectral Relaxation Method. The results obtained after varying Hartman number, Unsteadiness parameter, Reynolds number, Solutal and Thermal Grashof number on velocity, concentration, temperature and induction profiles are represented in form of graphs. Some of the application of this study are, when extracting the energy from earth crust that varies in length between five to ten kilometres and temperature in between 500° and 1000°, nano-fluids are employed to cool the machinery and equipment working under high friction and high temperature. This present study considers nanofluid acting as a coolant of such equipment as well as acting as a lubricant thus reducing the rate of wear and tear of the equipment. The copper-water increases the thermophysical properties thus increasing heat transfer coefficient and hence increasing cooling rate.

Keywords: Hydromagnetic, Spectral Relaxation Method, Collocation, Chemical Reaction, Non-Newtonian, Nanofluid, Thermophysical Properties

1. Introduction

Nanofluids can be defined as dilute suspensions of nanoparticles suspended in the base fluid forming the nanofluid and the particles suspended are less than 100 nanometre. From previous research and practicals done, nanofluids have been found to have an improved and enhanced thermopysical properties such as thermal diffusivity, thermal conductivity, viscosity, electrical conductivity and heat transfer by convectional currents compared to other base fluids such as oil, water to mention a few. Hence, nanotechnology is one of the most active research areas by most scientist today due to its vast applications. It's a multidisciplinary research area combining various fields of research including biology, chemistry, engineering and physics. Most importantly mathematical modelling can provide insights into the behaviours of nanostructural materials under different conditions and enhance the undestanding through new applications within this area.

Md S Alam (2013) [1] studied critical analysis on effects of magnetic Reynolds number on MHD Jeffery-Hamel flows. His main objective was to study the steady flow of a viscous

incompresible electrolyte in a convergent-divergent conduit in presence of an external applied constant magnetic field applied at an angle to the fluid flow direction. The governing equations for the considered fluid flow model was solved numerically using power series solution method to examine the instability of the problem using Hermite-Pade approximation technique. The change of angle values of the divergent conduit semi-angle, Reynolds number and type of the principal singularity on different selected magnetic Reynolds number are obtained and represented graphically. The observation was that when magnetic Reynolds number is increased, the bifurcation points of the solution also increase. The critical relationship between the non-parameters are discussed against the conduit angle. It was observed that as α increases it leads to Reynolds number to decrease and conversely and therefore this signify that α and Reynolds number are inversely proportional to each other.

Sheikholeslami, M *et al* [2] investigated magneto hydrodynamic nanofluid flow on non-parallel walls. In this, homotopy perturbation method was used to solve the arising models of equations and cu-water was used as the proposed nanofluid. The results were represented graphically. The validity of the used method was compared with numerical results obtained using a fourth order Runge-Kutta method to test its level of convergence. It was observed that increasing the Reynolds number lead to increment of the velocity boundary layer from the wall to the free stream region. It was still found that increasing nanoparticle volume lead to friction and Hartman number to increase. In this research the magnetic field was applied perpendicular to fluid flow direction, the effect of stretching walls was not taken into consideration and need to be considered.

Githaiga *et al* [3] investigated magnetohydrodynamics fluid flow past non-parallel walls in presence of constant pressure gradient and magnetic field which is uniform and applied normal to the fluid flow direction. The effect of Joule heating was taken into consideration. Similarity transformation was implemented to non-dimensionalise partial differential equations into ordinary differential equations. The results were represented graphically. It was found that increasing Joule heating led to increase in velocity and temperature profiles in the flow region. Also, increasing Hartman led to decrease of velocity. In this paper, there is a gap of nano-fluid and the effect of stretching non-parallel walls which needs to be considered.

Nagler [4] carried an investigation of Jeffery-Hamel non-Newtonian fluid flow with variable viscosity. The study which was carried out was on steady fluid flow. The method used on solving the arising equations was homotopy perturbation method and the results were represented in form of graphs and in tables. It was observed that increasing the friction coefficient led to decreament of velocity in the flow region, it was observed still that increasing the Reynolds number led to increase in normal velocity. The effects of any body force has not been factored in and thus it needs to be addressed. The energy equation which bring in the issue of internal heating needs to be taken into consideration and thus the present research will consider and address the said gap.

Onyango *et al* [5] studied unsteady Jeffrey-Hamel flow in the presence of oblique magnetic field with suction and injection. The equations formed were non-linear partial differential equations and similarity transformation was used to transform partial differential equations to ordinary differential equations. The arising ordinary differential equations were solved using an inbult bvp4c Matlab solver. The observations were velocity, temperature, and magnetic induction increases with the increase in the suction parameter and decrease in the wedge angle while velocity, temperature, and magnetic induction reduce with the increase in the injection parameter. The velocity, temperature and magnetic induction increase with the increase in the Hartmann number. In this study, effect of nanofluid is a gap which needs to be addressed.

Khan *et al* [6] investigated MHD Nanofluids in a Permeable Channel with Porosity including suction and injection. The perturbation numerical technique is used to obtain a closed-form solution for the velocity and temperature distributions. It was found that magnetic parameter retards the nanofluid motion whereas porosity accelerates it. They observed that increasing the nanofluid fraction volume led to velocity of the nanofluid to increase. Also, it was found that increasing permeability parameter increased the rate of injection and suction.

Moghimi *et al* [7] investigated Heat transfer of MHD flow over a Wedge with variable surface temperature. The study focused on the thermal distribution in the boundary layer of a wedge with a variable surface temperature. The governing equations of MHD flow for variable wall temperature conditions were converted to ODE by using similarity transformation and used collocation method to solve them. The observation was by increasing the wedge angle, the thermal boundary layer thickness decreased. The fluid considered was Newtonian fluids. Non-Newtonian fluids are industrial oriented. Thus fluid with variable viscosity i.e non-Newtonian is a gap which needs to be addressed since its industrial oriented. Furthermore, variable magnetic field, nanofluids and effects of stretching were not considered and needs to be taken into consideration.

This study has wide applications in engineering fields like increasing the cooling efficiency in cooling tower during geothermal power generation. In view from the important literature provided above, non-Newtonian fluids received Little attention despite being industry oriented. Moreso, Chemical reaction, variable thermal conductivity, viscous dissipation and variable magnetic field are areas which requires to be considered. This present study focuses on hydromagnetic non-Newtonian nanofluid flow past linearly stretching convergent-divergent conduit with chemical reaction since it has received little attention with spectral based relaxation numerical scheme.

This study focuses on expanding knowledge on geothermal power plant cooling efficiency and different numerical scheme on hydromagnetic nano-fluid flows. Nanofluids have wide applications in nuclear power production where it acts as a coolant. South Africa is the only African country producing

nuclear power commercially, other governments on the continent are exploring nuclear energy as a climate-friendly alternative to fossil fuels. In a pressurized water reactor (PWR) nuclear power plant system, the limiting process in the generation of steam is critical heat flux (CHF) between the fuels rods and the water, when vapor bubbles that end up covering the surface of the fuel rods conduct very little heat as opposed to liquid water. Using nanofluids instead of water, the fuel rods become coated with nanoparticles such as alumina, which actually push newly formed bubbles away, preventing the formation of a layer of vapor around the rod and subsequently increasing the CHF significantly. The use of nanofluids as a coolant could also be used in emergency cooling systems, where they could cool down overheat surfaces more quickly leading to an improvement in power plant safety. Over-reliance on fossils fuel in Africa has led to negative climatic conditions in the continent. Approximately 600 million people in the continent do not have access to electricity and around 900 million people lack access to clean cooking fuel as highlighted by [8] and [9] despite Africa having large potential production of geothermal power which is untapped. Nanofluid can enhance the rate of cooling in cooling tower during georthermal energy production. The present research considers hydromagnetic non-Newtonian nanofluid flow through stretching convergent-divergent conduit and chemical reactions. This research has taken into considerations the above stated gaps to enhance cooling rate in cooling tower in geothermal power production and has been addressed.

2. Mathematical Formulation

The figure below shows the geometry of the problem under consideration.

The fluid flow is laminar and the nanofluid considered in this study is of non-Newtonian type. There is no external applied electric field, Hall currents are negligible and the Viscosity is a non-linear function of the tangential direction θ and temperature T. The flow is axisymmetric and unsteady.

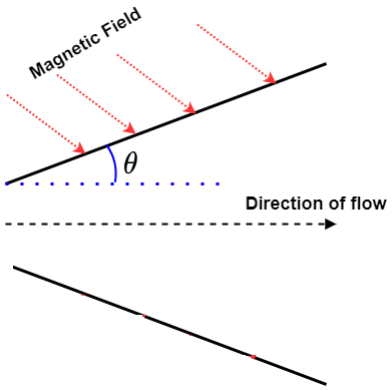

Figure 1. *Geometry of the problem.*

3. Governing Equations

The governing equations are conservation of mass, conservation of momentum, conservation of energy, magnetic induction equation and Concentration which are given respectively as:

Continuity equation:

$$\frac{1}{r}\frac{\partial(ru_r)}{\partial r} = 0 \tag{1}$$

Equation (1) represents the equation of continuity in cylindrical coordinates for a two-dimensional unsteady, laminar flow of an incompressible fluid whose motion is purely in radial direction i.e. the flow is axisymmetric.

The equation of continuity must be satisfied for any possible fluid flow.

Momentum equation:

$$\rho_{nf}\frac{\partial u_r}{\partial t} = -\frac{\partial P}{\partial r} - u_r\rho_{nf}\frac{\partial u_r}{\partial r} + \mu_{nf}[\frac{1}{r}\frac{\partial u_r}{\partial r} + \frac{\partial^2 u_r}{\partial r^2} - \frac{u_r}{r^2} + \frac{1}{r^2}\frac{\partial^2 u_r}{\partial\theta^2}] + \frac{1}{r^2}\frac{\partial\mu_{nf}}{\partial\theta}\frac{\partial u_r}{\partial\theta}$$

$$+g_r\rho_{nf}[\beta_T(T-T_\infty) + \beta_C(C-C_\infty)] - \rho_{nf}[\mu_e^2\sigma u_r(\mathbf{H}_\theta^* - \mathbf{H}_0 sin\alpha)(\mathbf{H}_\theta^* + \mathbf{H}_0 cos\alpha)] \tag{2}$$

Concentration equation:

$$\frac{\partial C}{\partial t} + u_r\frac{\partial C}{\partial r} = D_f(\frac{1}{r}\frac{\partial C}{\partial r} + \frac{\partial^2 C}{\partial r^2} + \frac{1}{r^2}\frac{\partial^2 C}{\partial\theta^2}) - k_r C \tag{3}$$

Initial conditions considered are as follows.

At the center line at $\theta = 0$:

$$\frac{\partial u_r}{\partial\theta} = 0, \frac{\partial T}{\partial\theta} = 0, \frac{\partial C}{\partial\theta} = 0. \tag{4}$$

on the walls of the plate at $\theta = \alpha$:

$$u_r = u_w = 0, \frac{\partial u_r}{\partial\theta} = -\gamma u(\theta), T = T_w, C = C_w \tag{5}$$

4. Thermophysical Properties

Nanofluids enhances the rate of effectiveness of heat transfer in fluids. Thermo-physical properties of the nano-fluids are essential for determining the heat transfer behaviours. For example, the thermal conductivity of the nanofluids depends on the volume fraction, base fluid material, particle material and the temperature. In this study we have considered copper-water nanofluid so that we the thermophysical properties of the base fluid is enhanced.

The following are the thermophysical expressions of the properties of the nano-fluids;

$$\sigma_{nf} = (1-\Psi)\sigma_f + \Psi\sigma_s \tag{6}$$

$$\rho_{nf} = (1-\Psi)\rho_f + \Psi\rho_s \tag{7}$$

$$\mu_{nf} = \frac{\mu_f}{(1-\Psi)^{2.5}} \tag{8}$$

$$(\rho C_p)_{nf} = (1-\Psi)(\rho C_p)_f + \Psi(\rho C_p)_s \tag{9}$$

$$k_{nf} = \frac{k_f[(k_s+2k_f) - 2\Psi(k_f-k_s)]}{k_s+2k_f+\Psi(k_f-k_s)} \tag{10}$$

$$(C_p)_{nf} = (1-\Psi)(C_p)_f + \Psi(C_p)_s \tag{11}$$

From equations (6) to (11) we can compute the following nanoparticles expressions:

$$\frac{\sigma_{nf}}{\rho_{nf}} = \frac{\sigma_f}{\rho_f}\left[\frac{(1-\Psi)+\Psi\frac{\sigma_s}{\sigma_f}}{(1-\Psi)+\Psi\frac{\rho_s}{\rho_f}}\right] = \frac{\sigma_f}{\rho_f}A \tag{12}$$

$$\frac{\mu_{nf}}{\rho_{nf}} = \frac{\mu_f}{\rho_f}\left[\frac{(1-\Psi)^{-2.5}}{(1-\Psi)+\Psi\frac{\rho_s}{\rho_f}}\right] = \frac{\mu_f}{\rho_f}C \tag{13}$$

$$\rho_{nf} = \rho_f\left[(1-\Psi)+\Psi\frac{\rho_s}{\rho_f}\right] = \rho_f M \tag{14}$$

$$\sigma_{nf} = \sigma_f\left[(1-\Psi)\sigma_f + \Psi\frac{\sigma_s}{\sigma_f}\right] = \sigma_f N \tag{15}$$

$$\frac{k*}{(C_p)_{nf}} = \frac{k_f}{(C_p)_f}\left[\frac{\frac{(k_s+2k_f)-2\Psi(k_f-k_s)}{k_s+2k_f+\Psi(k_f-k_s)}}{(1-\Psi)+\Psi\frac{(C_p)_s}{(C_p)_f}}\right] = \frac{k_f}{(C_p)_f}S \tag{16}$$

$$(C_p)_{nf} = (C_p)_f\left[(1-\Psi)+\Psi\frac{(C_p)_s}{(C_p)_f}\right] = (C_p)_f L \tag{17}$$

5. Similarity Transformation

From [4] and [3] among other researchers, the following similarity transformations are used to transform the specific equations of the fluid flow model from partial differential equations to ordinary differential equations.

$$u_r(r,\theta,t) = -\frac{Q}{r}\frac{1}{\delta^{m+1}}f(\theta) \tag{18}$$

$$\frac{\phi(\theta)}{\delta^{m+1}} = \frac{C-C_\infty}{C_w-C_\infty} \tag{19}$$

$$\frac{\omega(\theta)}{\delta^{m+1}} = \frac{T-T_w}{T_\infty-T_w} \tag{20}$$

$$\mu = \mu_0\theta^{c(n-1)} \tag{21}$$

$$\mathbf{H}_\theta(r,\theta,t) = -\frac{Q}{r}\frac{1}{\delta^{m+1}}\varphi(\theta) \tag{22}$$

$$\mathbf{H}_r(r,\theta,t) = -\frac{Q}{r}\frac{1}{\delta^{m+1}}\gamma(\theta) \tag{23}$$

Where $f(\theta)$ is the dimensionless velocity, $\omega(\theta)$ is dimensionless temperature, $\phi(\theta)$ is the dimensionless concentration, T_∞ is the temperature at the center of the tube, T_w is the temperature at the wall, C_∞ is the Concentration at the center of the tube, C_w is the concentration at the wall, δ is the time dependent length scale to cater for the unsteady state and m are arbitrary constant which is related to the wedge angle parameter.

On transforming equations (2) and (3) the equations reduces to:

$$\begin{aligned}\rho_{nf}(m+1)\frac{Q}{r}\frac{1}{\delta^{m+2}}\frac{d\delta}{dt}f = -\rho_{nf}(-\frac{Q}{r}\frac{1}{\delta^{m+1}}f)(\frac{Q}{r^2}\frac{1}{\delta^{m+1}}f) + \mu_0 c(n-1)[\frac{1}{r}(\frac{Q}{r^2}\frac{1}{\delta^{m+1}}f) + (\frac{-2Q}{r^3}\frac{1}{\delta^{m+1}}f)\\ -\frac{1}{r^2}(-\frac{Q}{r}\frac{1}{\delta^{m+1}}f) + \frac{1}{r^2}(-\frac{Q}{r}\frac{1}{\delta^{m+1}}f'')] + \frac{1}{r^2}(-\frac{Q}{r}\frac{1}{\delta^{m+1}}f')\mu_0 c(n-1)\theta^{c(n-1)-1}\end{aligned}$$

$$+g_r\rho_{nf}[\beta_T(T-T_\infty)+\beta_C(C-C_\infty)] - \rho_{nf}[\mu_e^2\sigma u_r(\mathbf{H}_\theta^* - \mathbf{H}_0 sin\alpha)(\mathbf{H}_\theta^* + \mathbf{H}_0 cos\alpha)] \tag{24}$$

$$-(C_W-C_\infty)\frac{m+1}{\delta^{m+2}}\frac{d\delta}{dt}\phi = D_f\frac{(C_w-C_\infty)}{r^2}\frac{\phi''(\theta)}{\delta^{m+1}} - k_r C \tag{25}$$

On simplifying and introducing the dimensionless parameters in equations (24) and (25) arising from the study as listed below:

$$\lambda = \frac{\rho_f\delta^m}{\mu_0 r^{m-1}}\frac{d\delta}{dt}, Re = \frac{Q\rho_f}{\mu_0}, Gr_T = \frac{g_r\rho_f}{\mu_o}r^3\beta_T(T_w-T_\infty),$$

$$Gr_C = \frac{g_r \rho_f}{Q\mu_o} r^3 \beta_C (C_w - C_\infty), Ha = \mu_e(\mathbf{H}_\theta^* - \mathbf{H}_0 sin\alpha(\mathbf{H}_\theta^* + \mathbf{H}_0 cos\alpha) r\sqrt{N}$$

$$\sqrt{\frac{\sigma_f}{\mu_0}}, Sc = \frac{\mu_0}{D_f \rho_f}, k_r = \frac{k_r \rho_f}{\mu_0} \frac{1}{C_w - C_\infty} \tag{26}$$

Where Re is Reynolds number, Ha is Hartmann number, Gr_T is Thermal Grashof number, Gr_c is solutal Grashof number, Sc is Schmidt number, λ is Unsteadiness parameter and k_r is Chemical reaction parameter in equations (26).

On substituting equations (26), (12) up to (17) in to equations (24) and equation (25), the equations reduces to:

$$(m+1) r^{m+1} \lambda M f = MRef^2 - c(n-1)\delta^{m+1} f^{''} - c(n-1)\theta^{c(n-1)-1}$$

$$\delta^{m+1} f^{'} + M\frac{Gr_T}{Q}\omega\delta^{m+1} + M\frac{Gr_C}{Q}\phi\delta^{m+1} + MNHa^2\delta^{m+1} f \tag{27}$$

$$-M(m+1)\lambda r^{m+1}\phi = \frac{M}{Sc}\phi^{''}\delta^{m+1} - Mk_r\delta^{2m+2} \tag{28}$$

The transformed Boundary conditions are as follows,

At the centerline $\theta = 0$ is

$$f(0) = -\frac{r u_\infty \delta^{m+1}}{Q}, f^{'}(0) = 0, \omega^{'}(0) = 0, \phi(0) = 0, \phi^{'}(0) = 0, \tag{29}$$

At the wall, $\pm\alpha$ is

$$f(\pm\alpha) = 0, f^{'}(\pm\alpha) = -\gamma f(\theta), \omega(\pm\alpha) = 0, \phi(\pm\alpha) = \delta^{m+1}, \varphi(\pm\alpha) = -\frac{r}{Q}\delta^{m+1} H_\infty \tag{30}$$

6. Numerical Solution Procedure Using Spectral Relaxation Model

This method is based on developing the system of non-linear ordinary differential equations using *Relaxation technique* and applying spectral collocation in the discretization of linearized system as explained by [10].

In the Relaxation method framework, the systems of non-linear ODEs equations (27) up to (28) are written as:

Momentum Equation:

$$L_1[f, \phi,] + N_1[f, \phi] = 0 \tag{31}$$

Concentration Equation

$$L_3[f, \phi,] + N_3[f, \phi] = 0 \tag{32}$$

Rearranging and simplifying equation (27), the equation reduces to:

$$(m+1) r^{m+1} \lambda M f - MRef^2 + c(n-1)\delta^{m+1} f^{''} + c(n-1)$$

$$\theta^{c(n-1)-1}\delta^{m+1} f^{'} - M\frac{Gr_T}{Q}\omega\delta^{m+1} - M\frac{Gr_C}{Q}\phi\delta^{m+1} - MNHa^2\delta^{m+1} f = 0 \tag{33}$$

Relaxation scheme for the equation (33) is:

$$c(n-1)\delta^{m+1} f_{r+1}^{''} + c(n-1)\theta^{c(n-1)-1}\delta^{m+1} f_{r+1}^{'} + \left[(m+1) r^{m+1}\lambda M - MNHa^2\delta^{m+1}\right] f_{r+1} =$$

$$MRef_r^2 + M\frac{Gr_C}{Q}\phi_r\delta^{m+1} + M\frac{Gr_T}{Q}\omega_r\delta^{m+1} \tag{34}$$

Considering concentration equation, equation (28), simplifying and re-arranging we have:

$$-M(m+1)\lambda r^{m+1}\phi - \frac{M}{Sc}\phi^{''}\delta^{m+1} + Mk_r\delta^{2m+2} = 0 \tag{35}$$

Relaxation scheme for equation (35) (Concentration equation)is:

$$\frac{M}{Sc}\delta^{m+1}\phi_{r+1}^{''} + M(m+1)\lambda r^{m+1}\phi_{r+1} = Mk_r\delta^{2(m+1)} \tag{36}$$

7. Spectral Collocation

The Method is based on approximating the solution of PDE by a polynomial function that satisfies ODE at a finite number of selected points called collocation points as [11]. The collocation method is applied using different types of basis functions such as polynomial, trigonometric etc. The choice for the basis function depends mostly on nature of ODEs and the problem geometry. The method uses solvers with low computational memory which makes it easy to implement. This method is one of the best numerical technique to solve BVP. The approximation solution $f(\theta)$ for the momentum equation is assumed to be the Lagrange interpolating polynomial of the form:

$$f(\theta) = \sum_{j=0}^{N} L_j(\theta) f_j \tag{37}$$

Where

$$L_j(\theta) = \prod_{\substack{i=0 \\ i \neq j}}^{N} \frac{\theta - \theta_i}{\theta_j - \theta_i} \tag{38}$$

is the Lagrange cardinal polynomial.

The grid points are the Chebyshev Gauss Lobatto points given by

$$\left\{ cos\left(\frac{i\pi}{N}\right) \right\}_{i=0}^{N} \tag{39}$$

in the interval $[-1, 1]$.

Appropriate linear transformation is applied to map the interval $[-1, 1]$ to the computational domain at $[0, \alpha]$.

The first derivative of $f(\theta)$ is approximated by:

$$f^{'}(\theta) = \sum_{j=0}^{N} L_j^{'}(\theta) f_j \tag{40}$$

$f^{'}(\theta)$ is evaluated at the collocation points as

$$f^{'}(\theta_i) = \sum_{j=0}^{N} L_j^{'}(\theta_i) f_j = \sum_{j=0}^{N} D_{ij} f_j = DF \tag{41}$$

where D is the chebyshev differential matrix as defined by [12] and

$$F = [f(\theta_0), f(\theta_1), f(\theta_2), ..., f(\theta_N)]^T \tag{42}$$

Higher order discrete derivatives are approximated using matrix multiplication.

$$F^{'} = DF, F^{''} = D^2F, F^{'''} = D^3F \tag{43}$$

The derivatives for ϕ at the collocation points is approximated in similar manner.

Substituting the discrete derivatives in the linear relaxation scheme, equations (34) and (36):

$$[c(n-1)\delta^{m+1}D^2 + c(n-1)\theta^{c(n-1)-1}\delta^{m+1}D] + [(m+1)r^{m+1}\lambda M - MNHa^2\delta^{m+1}]]F = R_1 \tag{44}$$

$$\left[M\mu_0 c(n-1)ReD + \left[M\mu_0 c(n-1)Re - NHa^2Q\right]\right] F = R_2 \tag{45}$$

$$\left[\frac{M}{Sc}\delta^{m+1}D^2 + M(m+1)\lambda r^{m+1}I\right] \Phi = R_4 \tag{46}$$

where R_1, R_2, and R_4 in equations (44), (45) and (46) are:

$$R_1 = MRef_r^2 + M\frac{Gr_C}{Q}\phi_r\delta^{m+1} + M\frac{Gr_T}{Q}\omega_r\delta^{m+1} \tag{47}$$

$$R_2 = M^2\rho_f G_{\theta T}\omega_r + M^2\rho_f G_{\theta C}\phi_r \tag{48}$$

$$R_4 = Mk_r\delta^{2(m+1)} \tag{49}$$

Transforming the boundary conditions using transformations equations (18) to (21), we have:
At the pipe wall, $\theta = \pm\alpha$

$$f(\pm\alpha) = 0, f^{'}(\pm\alpha) = -\gamma f(\theta), \phi(\pm\alpha) = \delta^{m+1} \tag{50}$$

At $\theta = 0$, the free stream interface is treated as a moving wall

$$f(0) = -\frac{u_\infty\delta^{m+1}}{Q}, f^{'}(0) = 0, \phi(0) = 0, \phi^{'}(0) = 0 \tag{51}$$

At the entry point, $(r = 0)$ the flow is not fully developed and we have

$$f(0) = -\frac{u_\infty \delta^{m+1}}{Q}, \phi(0) = 0, \phi^{'}(0) = 0 \tag{52}$$

At the exit point $(r = \infty)$, the gradients of all variables in the flow directions is equals to zero.

$$\frac{\partial f}{\partial r} = 0, \frac{\partial \phi}{\partial r} = 0 \tag{53}$$

8. Results and Discussions

Equations (44) up to (46) are solved using the MATLAB version 7.9.0 (R2021b) computer code under the boundary conditions equations (50) up to (53). The results obtained after running the code are presented in graphical form and discussions follow after varying various non-dimensional parameters.

8.1. Effects of Varying Reynolds Number on Velocity Profiles

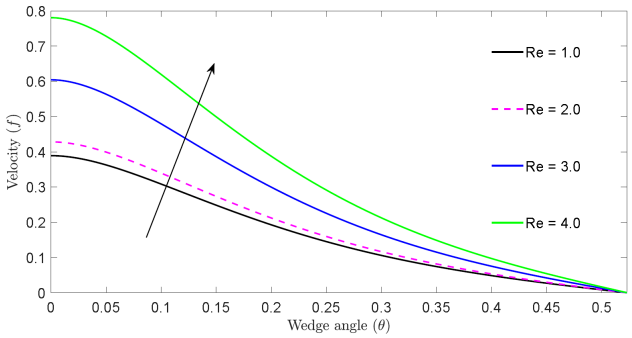

Figure 2. *Graph of dimensionless velocity profiles for different Reynolds.*

From figure 2, it is observed that on increasing the Reynolds number results to increase in velocity of the nano-fluid flow in the flow region. Reynolds number is the ratio of the inertial forces to viscous forces acting on the nano-fluid element. Increasing Reynolds number signifies that viscous forces are reducing and thus inertial forces dominates, viscous forces tends to oppose the motion of the flowing nano-fluid. Decreasing the viscous forces implies that velocity will absolutely increase because the velocity boundary layer formed does not really extend more in to the free stream region and hence the velocity increases.

The increase in velocity due to increasing Reynolds parameter increases the heat transfer coefficient. This is due to the fact that, on increasing the nanofluid velocity due to increase in Reynolds number, it leads to an increase in heat transfer coefficient. Hence, thermophysical properties of the nanofluid increases as the velocity of the nanofluid increases. This is as a result of, as the velocity of the nanofluid increases it leads to formation of many eddies. Consequently, this increases the rate of cooling in the cooling tower since nano-fluid increases the thermophysical properties and hence reducing the common cooling tower problems.

8.2. Effects of Varying Hartman Number on Velocity Profiles

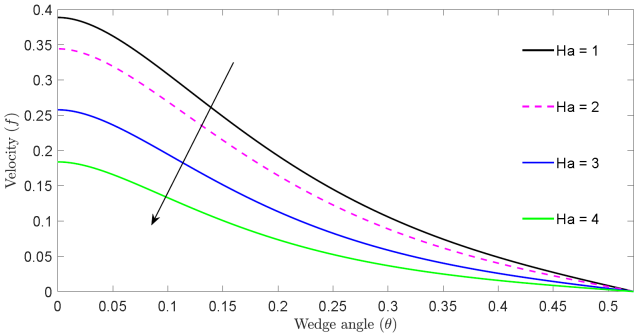

Figure 3. *Graph of dimensionless velocity profiles for different Hartman Number.*

Hartman parameter represents the ratio between electromagnetic force and viscous forces. Considering the velocity profile graph above, increasing the Hartman parameter leads to decrease of nano-fluid velocity in the flow region. The variable applied magnetic fluid which is applied at an angle to the flowing electrically conducting nano-fluid leads to production of Lorentz force due to effect of induced magnetic field. The induced force tends to act against the fluid flow direction and hence this retards the nano-fluid velocity and hence consequently leading to reduction of the fluid velocity in the flow region.

8.3. Effects of Varying Chemical Reaction on Concentration Profiles

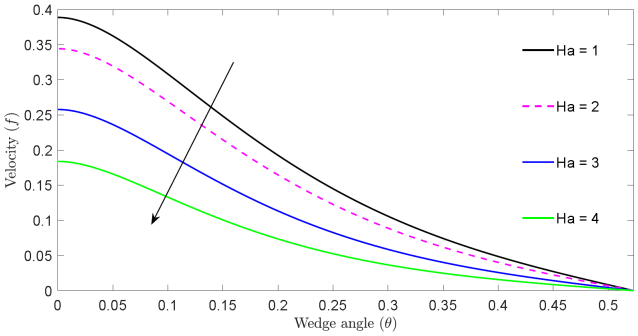

Figure 4. *Graph of dimensionless concentration profiles for different chemical reaction parameter.*

From the graph above, it shows that increasing chemical reaction parameter leads to reduction in concentration profiles.

This is as a result of, when you increase the chemical reaction, you reduce the amount of species in the fluid and this leads to species movement to decrease. During chemical reactions, the species are consumed as chemical reaction takes place. Also, the reduction of concentration is caused by the negative chemical reaction which reduces the concentration boundarly layer thickness and in turn increases the mass transfer. Chemical reaction is also known to reduce the concentration boundarly layer. This is as a result of that the reaction consumes the species reacting near the surface and hence this leads to reduction of the concentration gradient and the diffusion flux of the reacting species away from the wall.

8.4. *Effects of Varying Solutal Grashof Number on Velocity Profiles*

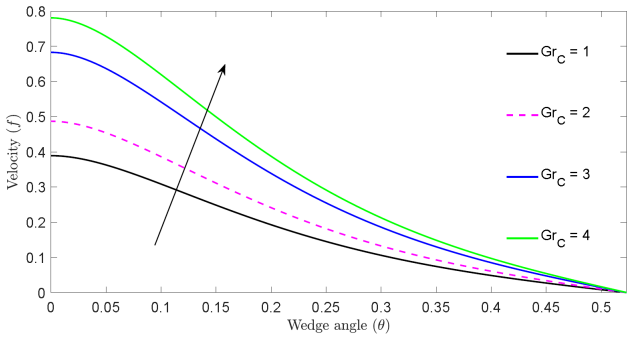

Figure 5. *Graph of dimensionless velocity profiles for different Solutal Grashof Number.*

The solutal Grasholf number represents the ratio between mass buoyancy forces to the viscous forces acting on a nano-fluid. Figure 5 shows that increasing solutal Grashof parameter leads to velocity to increase in the flow region. Increasing the Grashof number leads to reduction of viscous forces. Viscous forces tends to oppose the motion of the flowing nanofluid hence leading to velocity to increase in the flow region since bouyamcy forces are dominant. This increase in velocity as you increase Solutal Grashof leads to increased heat transfer coefficient thus leading to more efficient cooling since increasing velocity increases the heat transfer.

8.5. *Effects of Varying Unsteadiness Parameter, λ on Velocity Profiles*

Unsteadiness parameter, λ caters for the unsteady state of the nano-fluid flow and the time-dependent scale which caters for the unsteady state of the study being considered. From figure 6 increasing the unsteadiness parameter leads to fluid velocity to decrease in the flow region.

From the definition of unsteadiness parameter, $\lambda = \frac{\rho_f \delta^m}{\mu_0 r^{m-1}} \frac{d\delta}{dt}$, we observe that the unsteadiness parameter and time-dependent lengths scale have direct relation. From $u_r(r,\theta,t) = -\frac{Q}{r}\frac{1}{\delta^{m+1}} f(\theta)$, we see that time -dependent length scale have an inverse relationship signifying that when unsteadiness parameter increases then the nano-fluid velocity decreases. This shows increasing the unsteadiness parameter leads to reduction of velocity in the nano-fluid flow region.

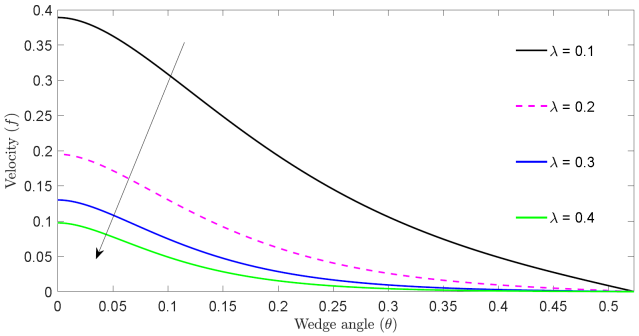

Figure 6. *Graph of dimensionless velocity profiles for different unsteadiness parameter, λ.*

8.6. *Effects of Varying Schmidt Number on Concentration Profiles*

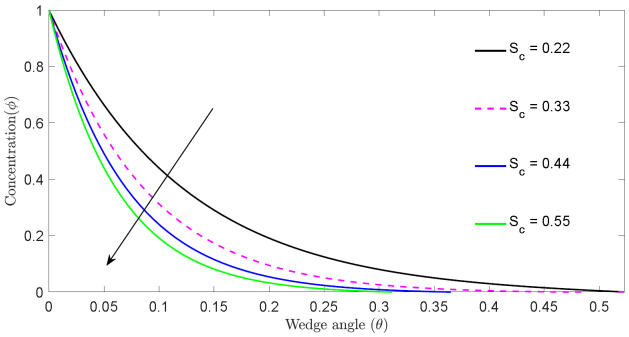

Figure 7. *Effects of varying Schmid number on concentration profiles.*

This number gives the ratio of the momentum diffusivities (kinetic viscosity) to mass diffusivities. From the graph above, it can be inferred that, increasing Schmid number leads to a decrease in concentration profiles. Increasing Schmid number results in decrease in molecular diffusivity, this in turn leads to reduction in the concentration boundary layer thickness. Practically, it has been proved that Schmid number is always inversely proportional to concentration, thus on increasing Schmid number leads to a decrease in the concentration in the nano-fluid flow region. On decreasing concentration profiles, this shows no scale formed along the pipes and hence cooling remains to be efficient and no build up pressure which could result in explosion.

9. Conclusions

1. It is observed that on increasing the Reynolds number results to increase in velocity of the nano-fluid flow in the flow region.
2. It is observed that ncreasing the Hartman parameter leads to decrease of nano-fluid velocity in the flow region. The variable applied magnetic fluid which is

applied at an angle to the flowing electrically conducting nano-fluid leads to production of Lorentz force due to effect of induced magnetic field.

3. It shows that increasing chemical reaction parameter leads to reduction in concentration profiles. This is as a result of, when you increase the chemical reaction, you reduce the amount of species in the fluid and this leads to species movement to decrease.
4. It is observed that increasing solutal Grashof parameter leads to velocity to increase in the flow region. Increasing the Grashof number leads to reduction of viscous forces.
5. It is inferred that, increasing Schmid number leads to a decrease in concentration profiles. Increasing Schmid number results in decrease in molecular diffusivity, this in turn leads to reduction in the concentration boundarly layer thickness.
6. It is observed that increasing the increasing the unsteadiness parameter leads to fluid velocity to decrease in the flow region.

10. Validation

The results of this study were validated against [3], in absence of chemical reaction, the results are in agreement.

Abbreviations

MHD	Magnetohydrodynamics
ODE	Ordinary Differential Equation
PDE	Partial Differential Equations
BVP	Boundary Value Problem
u_θ	Tangential Velocity, Rad ($rad\ s^{-1}$)
u_r	Radial Velocity, Meters (ms^{-1})
r	Radius of the Tube, Meters (m)
t	Time, Seconds (s)
B_0	Applied Magnetic Field, Tesla (T)
κ	Variable Thermal Viscosity
T	Temperature, Kelvin (K)
T_∞	Temperature at the Center, Kelvin (K)
T_w	Temperature at the Wall, Kelvin (K)
C	Concentration, Mole Per Cubic Meter mol/m^3
C_∞	Concentration at the Center, Mole Per Cubic Meter mol/m^3
C_w	Concentration at the Wall, Mole Per Cubic Meter mol/m^3
D_m	Concentration Diffusion Parameter, (m^2s^{-1})
k_r	Chemical Reaction Coefficient, (Ms^{-1})
Q	Discharge, (m^3s^{-1})
$f(\eta)$	Dimensionless Velocity
P	Pressure, (Nm^{-2})
m	Arbitrary Constant
I	Electric Current, Ampere (A)
J	Electric Current Density, (Am^{-2})
$\overrightarrow{B}$	Magnetic Vector
g	Gravitational Force, (Nm^2kg^{-2})
q_h	Heat Flux, (Wm^{-2})
q_m	Mass Flux, ($kg\ m^{-2}s^{-1}$)
Re	Reynolds Number
Ha	Hartmann Number
Gr_T	Thermal Grashof Number
Gr_c	Concentration Grashof Number
Sc	Schmidt Number
λ	Unsteadiness Parameter
α	Thermal Diffusion Rate
β^c	Volumetric Concentration Expansion, ($kg\ m^{-3}$)
β^t	Volumetric Thermal Expansion, Kelvin K^{-1}
ϕ	Chemical Reaction Parameter Ms^{-1}
δ	Time-dependent Length Scale, M
η	Dimensionless Radius
λ	Unsteadiness Parameter
μ	Fluid Viscosity, $kg\ m^{-1}s^{-1}$
ρ_nf	Nano-Fluid Density, kgm^{-3}
κ	Thermal Conductivity, Wm^{-1}K^{-1}
τ	Shear Stress, Nm^{-2}
σ	Electrical Conductivity, $\Omega^{-1}m^{-1}$
τ_w	Skin Shear Stress, Nm^{-2}
θ	Wedge Angle, Rad
$\omega(\theta)$	Dimensionless Temperature
$\phi(\theta)$	Dimensionless Concentration

ORCID

0009-0007-7595-7017 (Paul Wachira Githaiga)

Acknowledgments

Authors are grateful to the P an African University Institute for Basic Sciences, Innovation and Technology(PAUSTI) for their support throughout the conduct and execution of this present study.

Conflicts of Interest

We declare that we have no conflicts of interest.

References

[1] Md S Alam. (2013) "Critical analysis of the influence of magnetic reynolds number on mhd jeffery−hamel flows", Journal of Naval Architecture and Marine Engineering, Academic publisher, China. vol. 9(5), 31-46.

[2] Sheikholeslami, M and Mollabasi, H and Ganji, DD. (2015) "Analytical investigation of MHD Jeffery–Hamel nanofluid flow in non-parallel walls", International Journal of Nanoscience and Nanotechnology, Iranian Nanotechnology Society, Iran. vol. 11(4), 241-248.

[3] Githaiga, Paul Wachira and Kinyanjui, Mathew Ngugi and Giterere, Kangethe and Kogora, Phineous Roy. (2018) "Magneto Hydrodynamics Fluid Flow in Convergent-Divergent Conduit", *International Journal of Engineering Science and Innovative Technology(IJESIT)*, vol. 7, 1-10.

[4] Nagler, J. (2017) "Jeffery-Hamel flow of non-Newtonian fluid with nonlinear viscosity and wall friction", *Applied Mathematics and Mechanics*, Springer, Germany. vol. 38, 815-830.

[5] Onyango, Edward Richard and Kinyanjui, Mathew Ngugi and Kimathi, Mark and Uppal, Surindar M. (2020) "Unsteady Jeffrey-Hamel Flow in the Presence of Oblique Magnetic Field with Suction and Injection", *Applied and Computational Mathematics*, Science Publishing Group. vol. 9(1), 1-13.

[6] Khan, Ilyas and Alqahtani, Aisha M. (2019) "MHD Nanofluids in a Permeable Channel with Porosity", *Symmetry*, Multidisciplinary Digital Publishing Institute. vol. 11(3), 378.

[7] Moghimi, Seyed Morteza and others. (2023) "Heat Transfer of MHD Flow over a Wedge with Surface of Mutable Temperature", *Authorea Preprints*, Authorea. vol. 11(3), 4.

[8] Soumahoro, Moussa and Kinkoh, Hubert and Aikins, Enoch Randy and Louw-Vaudran, Liesl. (2023) "Tracking Africa's implementation of Agenda 2063 milestones", *ISS Peace and Security Council Report*, Institute for Security Studies (ISS). vol. 155(3), 11-14.

[9] Arthur, Kingsley K and Asongu, Simplice A and Darko, Peter and Ansah, Marvin O and Adom, Sampson and Hlortu, Omega. (2023) "Financial crimes in Africa and economic growth: Implications for achieving sustainable development goals (SDGs)", *Journal of Economic Surveys*, Wiley Online Library.

[10] Boyd, John P. (2001) "Chebyshev and Fourier spectral methods", Courier Corporation.

[11] Kaigalula, Victor and Mutua, Samuel. (2024) "Soret and Dufour Effects on MHD Fluid Flow Through a Collapssible Tube Using Spectral Based Collocation Method", Applied and Computational Mathematics.

[12] Trefethen, Lloyd N Spectral methods in MATLAB, SIAM. (2000).